Characterization of PAN/PANI-DBSA blend nanofibers produced by electrospinning method

WEI PAN*, QI ZHANG, YAN CHEN
School of Materials and Chemical Engineering, Zhongyuan University of Technology, Zhengzhou 450007, P. R. China

In this study, composite nanofibers of polyaniline doped with dodecylbenzene sulfonic acid (PANI-DBSA) and polyacrylonitrile (PAN) were prepared via an electrospinning process. The surface morphology, thermal properties and crystal structure of PAN/PANI-DBSA nanofibers are characterized using Fourier transform infrared spectroscopy (FT-IR), wide-angle x-ray diffraction (WAXD), scanning electron microscopy (SEM), Thermo gravimetric analyses (TGA) and differential scanning calorimetry (DSC). SEM images showed that the morphology and diameter of the nanofibers were affected by the weight ratio of blend solution. FT-IR, DSC and TGA demonstrated that there were strong intermolecular hydrogen bonds between the molecules of PAN and PANI-DBSA.

(Received October 25, 2010; accepted November 29, 2010)

Keywords: Electrospinning, PAN, PANI-DBSA, Nanofibers

1. Introduction

One-dimensional nanostructured materials with a variety of forms, such as nanotubes, nanowires, nanobelts, and nanofibers, are of great interest due to their unique properties and intriguing applications in many fields. Among various methods to prepare these materials, electrospinning is currently one of the most versatile and promising processes for producing continuous nanofibers for both fundamental and application-oriented research mainly due to its capability and feasibility in generating large quantities of nanofibers with well-defined surface topologies at relatively low cost [1-3]. Polyaniline (PANI) is one of the most promising conducting polymers due to its straightforward polymerization and excellent chemical stability combined with relatively high levels of conductivity. Volumes of researches focusing on conducting PANI have been made in developing soluble or melt-processable PANI, and significant progresses have been made in this area since the last decades [4-6].

The counter-ion induced solubility of PANI is a successful attempt to solve the processing problem of PANI. For example, PANI doped with organic acids containing long alkyl chains such as camphor sulfuric acid (CSA) or dodecylbenzene sulfonic acid (DBSA) could be soluble in some common solvents. The soluble PANI was then usually blended with polar polymer matrixes, such as PMMA [7-9], PA [10] and PANI doped by DBSA (PANI-DBSA) with PS [11], EPDM [12], PVC [13], PI [14] and SEBS [15] have been report.

Polyacrylonitrile (PAN) is one of the most important fiber-forming polymers and has been widely used because of its high strength, abrasion resistance, and good insect resistance [16, 17]. However, the PAN based conducting blends has not been explored, which should be a competitive system for making conductive fiber.

In this work, soluble polyaniline doped with dodecylbenzene sulfonic acid (PANI-DBSA) was used to blend with polyacrylonitrile (PAN) via solution mixing. The blend solution was spun into the composite fiber via electrospun technique. The conductivity, property as well as morphology of the PANI-DBSA/PAN composite nanofibers were investigated.

2. Experimental

Polyaniline (PANI) was synthesized by the oxidative polymerization of aniline in acidic media. 10 ml of aniline was dissolved in 300 ml of 1M HCl and kept at 0 □, 11.4 g of $(NH_4)_2S_2O_8$ was dissolved in 200 ml of 1M HCl also at 0 □ and added dropwise under constant stirring to the aniline/HCl solution over a period of 20 mins. The resulting dark green solution was maintained under constant stirring for 24 hrs. filtered and washed with water before being added to 500 mL of 1M $(NH_4)OH$ solution. After an additional 24 hrs， the solution was filtered and a deep blue emeraldine base from of polyaniline was obtained (PANI-EB). PANI-EB was added to DMF with stirring at 60 °C. This solution was stirred for 12 h and then filtered using absorbent cotton to remove any particulate matter. A DMF solution of EB was doped with DBSA, and the green conducting form was obtained. Different amounts of PAN were then poured into the doped PANI over a period of 4 h, with magnetic stirring, to obtain a homogeneous solution.

Composite solutions were fed through a capillary tip (diameter = 0.5mm) using a syringe (30 ml). The anode of the high voltage power supply was clamped to a syringe needle tip and the cathode was connected to a metal

collector. During electrospinning, the applied voltage was 14 kV, the distance between the tip and collector was 17 cm, and the flow rate of the spinning solution was 1 ml/h.

The diameter and morphology of the electrospun PANI-DBSA/PAN composite fibers were determined by a JSM-5610 scanning electron microscope (SEM, Japan). Wide angle X-ray diffraction was carried out using a BRUKER-AXC08 X-ray diffractmeter and filtered CuKα radiation. The diffraction patterns of the composite fibers of the PANI-DBSA and PAN were obtained by scanning the samples in an interval of 2θ = 10-60 degrees. Fourier transform infrared (FTIR) spectra were collected from a FTIR spectrometer (Nicolet 560) in the wavenumber range of 4000–700 cm^{-1}. Thermal properties of electrospun fibers were evaluated using differential scanning calorimetry (DSC) from 40 to 400□ at a heating rate of 20 □ min^{-1} in nitrogen environment. The thermal stability of composite fibers was investigated by TGA (Du Pont l090) under air atmosphere.

3. Results and discussion

Nanofiber diameter is typically influence by the viscosity and conductivity of the spinning solution. To understand the relationship between nanofiber diameter and PANI-DBSA concentration, the viscosity and conductivity were measure for all electrospinning solution and are shown in Fig. 1. The viscosity of the spinning solution increased with the addition and increasing amount of PANI-DBSA (i.e., form about 3927 mP for neat PAN solution to about 4265 mP for spinning solution containing 15 wt% PANI-DBSA), while the conductivity of spinning solution ranged between about 0.127 and 0.49 mS cm^{-1}.

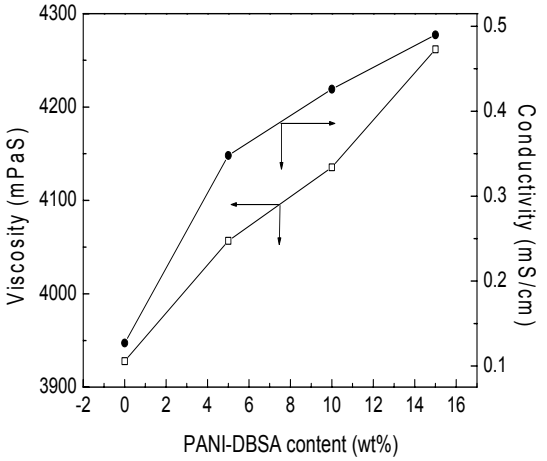

Fig. 1. The conductivity and viscosity of electrospinning solution as a function of PANI-DBSA content.

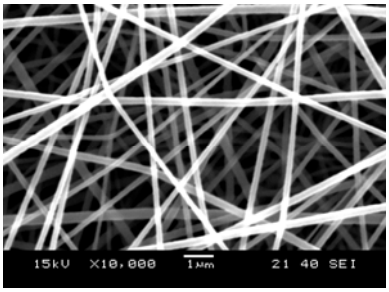

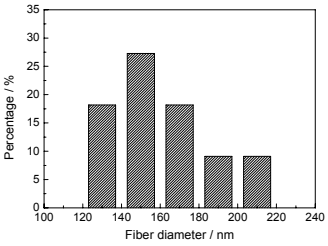

a

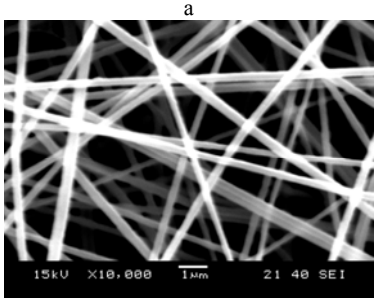

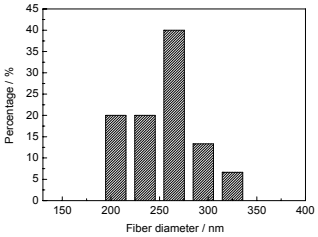

b

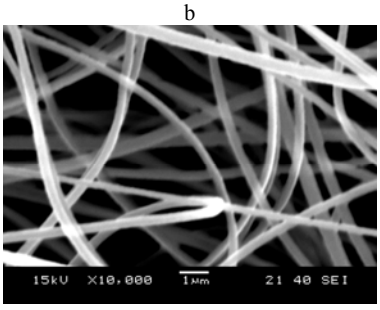

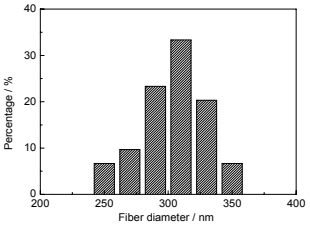

c

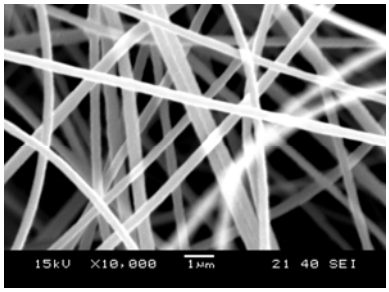

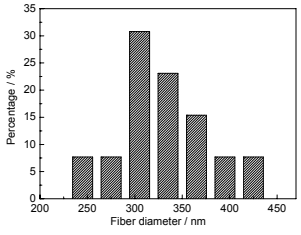

d

Fig. 2. SEM images of PANI-DBSA/PAN composite nanofibers with different PANI-DBSA contents. (a) 0 wt% (pure PAN), (b) 5 wt%, (c) 10 wt% and (d) 15 wt%.

Fig. 2 shows SEM images and diameter distribution curves of PANI-DBSA/PAN composite nanofibers electrospun from 12 wt% PAN solutions with different PANI-DBSA concentrations (0, 5, 10, and 15 wt %) at a fixed voltage of 14 kV. It is seen that all fibers are relatively uniform and randomly oriented, forming an interwoven network on the substrate. Defects, such as beads or fibers with 'beads on a string' morphology, can seldom be seen in all fibers with different PANI-DBSA content. The average fiber diameter of pure PAN is about 170 nm. When the PANI-DBSA content increases from 5 to 10 and 15 wt%, the average fiber diameter becomes gradually larger from 260 to 310 and 340 nm, respectively.

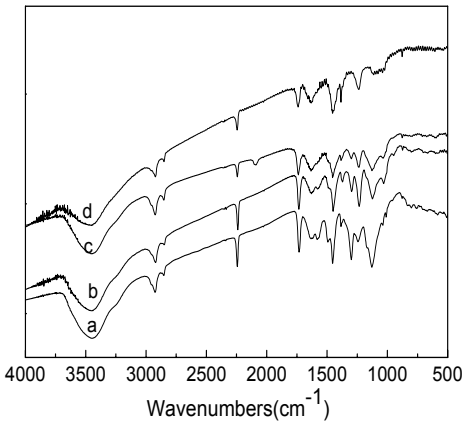

Fig. 3. FT-IR spectra of PANI-DBSA/PAN nanofibers with different PANI-DBSA contents (a) 0 wt% (pure PAN),(b) 5 wt %, (c) 10 wt%, and (d) 15 wt%.

FT-IR spectra of the pure PAN and PAN-DBSA/PAN nanocomposites with different PANI-DBSA loadings were recorded in the range 4000-400 cm^{-1}. All of the FT-IR spectra, Fig. 3, exhibit the PAN characteristic peaks such as the stretching vibration of nitrile groups (-CN-) at 2244 cm^{-1} and the stretching vibration and bending vibration of methylene (-CH_2-) peaks at 2930 and 1453 cm^{-1}, respectively. The peak at 1670 cm^{-1} is due to the oxidation of the as-received PAN in air, which results in the formation of carboxyl (C=O) groups [18, 19]. The peaks at 1251 and 1360 cm^{-1} are assigned to the aliphatic CH group vibrations of different modes in CH and CH_2, respectively. The positions of these peaks in composite nanofibers shift to slightly lower values due to the interaction between PAN molecules and zinc ions. The peak intensity of the C=O stretching observed at about 1670 cm^{-1} increases greatly with increase in PANI-DBSA concentration. These phenomena indicate that PANI-DBSA and possibly the PAN molecules interact with the solvent DMF [20].

DSC thermograms of pure PAN and PANI-DBSA nanofibers are in the range of 40-400℃ presented in fig.4. All nanofiber samples exhibit a relatively large exothermic peak. With increase in PANI-DBSA content, the exothermic peak became weaker and shift to higher temperatures. This peak can result from a combination of three principal reactions, namely dehydrogenation, instantaneous cyclization and crosslinking reactions, which are exothermic in nature [21]. Among these three reactions, the predominant process is the instantaneous cyclization of the nitrile groups into an extended conjugated ring system. The fast reaction of PAN nanofibers in nitrogen may be due to the facile formation of free radicals on the nitrile groups and subsequent recombinations between the radicals intermolecularly or intramolecularly [22]. Increases in peak temperature for PAN/PANI-DBSA composite nanofibers may be caused by the inhibiting effect of PANI-DBSA, which hinder the recombinations between the radicals

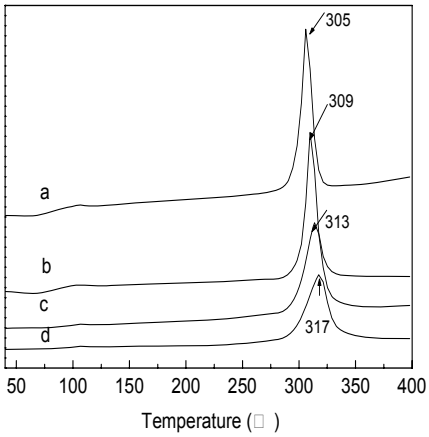

Fig. 4. DSC curves of PANI-DBSA/PAN nanofibers with different PANI-DBSA contents. (a) 0 wt% (pure PAN),(b) 5 wt %, (c) 10 wt%, and (d) 15 wt%.

The crystalline properties of electrospun fibers are important when the materials are designed and fabricated for commercial applications. In order to investigate the crystalline structure of the PAN and PANI-DBSA in the electrospun PAN nanocomposite fibers, XRD measurements were performed.

Fig.5 shows the XRD patterns of the as-received pure PAN powder and PAN/PANI-DBSA nanofibers with different PANI-DBSA content. The XRD pattern of the as-received pure PAN powder shows a diffraction peak at 2θ =17°. We found the crystallinity of pure PAN nanofibers was lower than PAN powder. This phenomenon confirmed the electrospinning retarded the crystallization process of polymer, which did not lead to the development of the crystalline microstructure of electrospun fiber. The reason for the retardation could be explained as following. During electrospinning, the stretched molecular chains of the fiber solidified rapidly at high elongate rates, which significantly hindered the formation of crystals.

If there were no or weak interaction between PAN and PANI-DBSA in the blend fibers, and XRD patterns would be expressed as simple mixed patterns of PAN and PANI-DBSA with the same ratio as those for mechanical blending. In fact, the intensity of the peak at 2θ =17° in the composite nanofibers increased with the decreased of PAN content. These observations indicate a large influence of PANI-DBSA on the crystallinity of PAN in the composite fibers and a strong interaction between the PANI-DBSA and the PAN matrix.

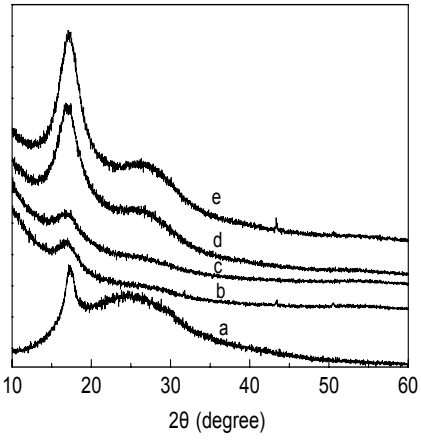

Fig. 5. XRD patterns of the (a) as-received pure PAN powder and PAN/PANI-DBSA composite nanofibers with different PANI-DBSA contents (b) 0 wt% (pure PAN fiber), c) 5 wt%, (d) 10 wt%, (e) 15 wt%.

TGA curves in Fig. 6 showed the dependence of thermal stabilities of PANI-DBSA/PAN nanofibers on PANI-DBSA content. There are two obvious weight loss peaks at 250-270 ºC and 550-580 ºC in the TGA curves. The first weight loss is caused by decarboxylation of the methylacrylate in PAN and the second weight loss is due to thermo-oxidative degradation of PAN macromolecular chains.

For PANI-DBSA/PAN composite, the temperature of the first weight loss peak becomes higher when with more content of PANI-DBSA, while the temperature of the second weight loss decreased with increasing PANI-DBSA content. The better thermal stability of the blend than either of pure PANI-DBSA and pure PAN before 500 ºC could be considered as additional evidence of interactions between PANI-DBSA and PAN. However, the hydrogen bonding will be destroyed at higher temperature and the decomposition of PANI-DBSA may accelerate the degradation of PANI-DBSA/PAN composite. This may be the reason that the peak temperature of thermo-oxidative degradation of the blends gets a little lower with the increasing component of PANI-DBSA.

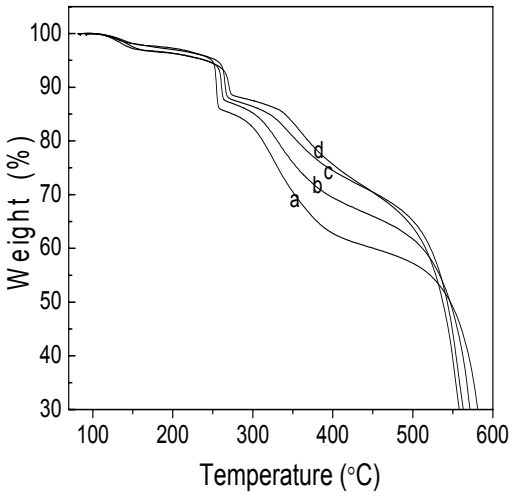

Fig. 6. TGA curves of of PAN/PANI-DBSA nanofibers with different PANI-DBSA contents. (a) 0 wt% (pure PAN),(b) 5 wt %, (c) 10 wt%, and (d) 15 wt%

4. Conclusions

Various PAN/PANI-DBSA composite fibers were prepared by electrospinning composite solutions containing PANI-DBSA and polyacrylonitrile (PAN) in N, N dimethylformamide (DMF). The effects of the blend weight ratio on structure and morphology of the fibers were investigated for the first time. The result indicated that the average diameter of the fiber gradually increased with the increasing of PANI-DBSA content. FTIR, DSC and TGA curves reveal that there are interactions among PAN and PANI-DBSA. These interactions have profound effects on the thermal properties of nanofibers. It is found that the amount of PANI-DBSA could affect the thermal stabilities of PAN. The PAN/PANI-DBSA composite nanofiber is thermally more stable than the corresponding neat PAN fiber.

References

[1] D. Li, Y. N. Xia, Advanced Materical reaearch **16**, 1151 (2004).

[2] A. Greiner, J. H. Wendorff, Angewandte Chemie International Edition **46**, 5670 (2007).

[3] J. M. Deitzel, J. Kleinmeyer, D. Harris, Polymer **42**, 261 (2001).

[4] Y. Wusheng, E. Ruckenstein, Synthetic Metals **108**, 39 (2000).

[5]Y. Guoli, K. Noriyuki, S. J. Su, Synthetic Metals **129**, 173 (2002).

[6] A. T. Royappa, D. D. Steadman, T. L. Tran, Synthetic Metals **123**, 273 (2001).

[7] M. E. Leyva, G. M. Barra, M. M. Gorelova, Journal of Appled Polymer Science **80**, 626 (2001).

[8] G. M. Barra, M. E Leyva, B. G. Soares, L. H. Mattoso, Journal of Appled Polymer Science **82**, 114 (2001).

[9] C. Y. Yang, Y. Cao, P. Smith, A. J. Heeger, Synthetic Metals **53**, 293 (1993).

[10] L. Zhang, Y. Long, Z. Chen, Advanced Functional Materials **14**, 693 (2004).

[11] E. Segal, Y. Haba, M. Narkis, Journal of Polymer Science Part B: Polymer Physics **39**, 611 (2001).

[13] R. K. Paul, C. K. Pillai, Journal of Applied Polymer Science **80**, 1354 (2001).

[14] L. Liangcai, W. Ming, S. Huoming. Polymers for Advanced Technologies **12**, 720 (2001).

[15] M. O. B, Guilherme, B. J. Livio, L. O. Rodrigo, Europe Polymer Journal **40**, 2017 (2004).

[16] R. B. Mathur, O. P. Bahl, P. Sivaram, Curr. Sci. **62**, 662 (1992).

[17] M. Panapoy, A. Dankeaw, B. Ksapabutr, Int. J. Sci. Technol. **13**, 11 (2008).

[18] M. A. Phadke, S. S. Kulkarni, S. K. Karode, D. A. Musale, J. Polym. Sci. Part B: Polym. Phys. **43**, 2074 (2005).

[19] X. Qu, T. Guan, G.. Liu, Q. She, J. Appl. Polym. Sci. **97,** 348 (2005).

[20] P. Cousin, P. Smith, J. Polym. Sci. Part B: Polym. Phys. **32**, 459 (2003).

[21] C. Kim, Y. Jeong, B. T. Nhu-Ngoc, K. S. Yang, M. Kojima, Y. A. Kim, M. Endo, J. W. Lee, Small **3,** 91 (2007).

[22] L. W. Ji, C. Saquing, S. A. Khan, X. G. Zhang**,** Nanotechnology **19,** 1 (2008).

*Corresponding author: panwei@zzti.edu.cn